European Journal of Mechanics / B Fluids 114 (2025) 204340

Contents lists available at ScienceDirect

European Journal of Mechanics / B Fluids

journal homepage: www.elsevier.com/locate/ejmflu

Evaluating the effects of bronchioles simplification on respirable dust deposition: A combined experimental and CFD-DPM analysis approach

Ahmed Aboelezz [a],*, Wei-Chung Su [b], Mohammad Rezaee [c], Pedram Roghanchi [d]

[a] Department of Mechanical Engineering, University of Maine, Orono, 04469, ME, USA
[b] Department of Environmental Science, Baylor University, Waco, 76798, TX, USA
[c] Department of Energy and Mineral Engineering, The Pennsylvania State University, University Park, 16802, PA, USA
[d] Department of Mining Engineering, University of Kentucky, Lexington, 40508, KY, USA

ARTICLE INFO

Keywords:
CFD
Wind tunnel testing
PIV
Respirable coal dust
Coal mines
Black lung disease

ABSTRACT

The resurgence of black lung disease among miners underscores the pressing need to enhance our understanding of respirable dust deposition mechanisms. This paper critically evaluates the widespread practice of simplifying bronchioles geometries in dust deposition studies, a method commonly employed but often without adequate consideration of its impact on particle–wall interactions and subsequent deposition calculations. Through the integration of experimental setups with computational simulations, this study investigates the behavior of respirable coal dust using Particle Image Velocimetry (PIV) and a specially designed dust wind tunnel equipped with both complex and simplified bronchioles models. Further, this research employs Computational Fluid Dynamics-Discrete Phase Model (CFD-DPM) simulations within ANSYS Fluent, incorporating these diverse models to assess the ramifications of geometrical simplification. A bronchioles wall observing model was introduced to enhance the simulation's realism by more accurately representing the dynamic interactions between dust particles and bronchioles wall surfaces. The complex model showed about 1.5×higher dust deposition compared to the simplified model. This difference was partially attributed to its larger surface area, with a surface area ratio of approximately 1.92. A correction factor based on this ratio was proposed to enhance the predictive capability of simplified models. This approach not only sheds light on the significant influences of particle size and airway geometry on dust deposition but also challenges the reliability of simplified models in replicating these complex processes. This work contributes valuable insights into improving occupational health safety measures in mining and related industries, highlighting the need for careful consideration of model selection and its implications in environmental health research.

1. Introduction

Respirable dust bronchioles deposition is pivotal in the development of pulmonary diseases, such as black lung disease, which predominantly impacts miners. Recent years have witnessed an unexpected resurgence in black lung disease cases, prompting a renewed examination of its underlying mechanisms [1]. The bronchioless serve as the primary interface between the body and the external environment through the act of breathing. They possess a vast surface area and an exceptionally thin air-blood barrier, making them highly susceptible to particles in the inhaled air. The interaction between these particles and the bronchioles tissue can have harmful health effects if the particles are toxic, such as those encountered in mining environments. Conversely, this interaction can be leveraged beneficially in medical treatments using therapeutic aerosolized drugs. Accurate estimation of the dosage and deposition sites within the respiratory tract is crucial for understanding the subsequent biological responses. This requires a solid grasp of the fundamental physics governing particle motion and the engineering principles involved, which are central themes in this field of study [2]. In recent years, Computational Fluid Dynamics (CFD) has emerged as a powerful tool for studying particle transport and deposition within the human respiratory system. By simulating airflow and particle interactions, CFD provides critical insights into the behavior of particles in various regions of the airway. This approach has been instrumental in predicting deposition patterns and understanding how factors such as particle size, shape, and breathing dynamics influence regional deposition within the respiratory tract. CFD modeling is particularly valuable in developing strategies to mitigate bronchioles deposition in high-risk environments, such as coal mines, where the prevalence of black lung disease remains a persistent concern [3].

* Corresponding author.
E-mail address: ahmed.aboelezz@maine.edu (A. Aboelezz).

https://doi.org/10.1016/j.euromechflu.2025.204340
Received 17 April 2025; Received in revised form 4 June 2025; Accepted 29 July 2025
Available online 14 August 2025

Recent advancements in respiratory research have highlighted critical factors influencing particle deposition in the human respiratory tract. Studies utilizing anatomically accurate upper respiratory tract models have demonstrated that coal dust deposition varies significantly with particle size and labor intensity, with higher respiratory flow velocities, induced by strenuous activity, increasing deposition fractions in critical regions such as the pharynx and larynx [4]. Similarly, aging has been shown to affect airflow dynamics and particle deposition patterns, as computational studies reveal that reduced bronchioles diameters with age lead to increased airflow velocity and a shift in deposition predominantly to the upper airways [5]. Combined in vitro experiments and CFD simulations further emphasize the role of airflow turbulence and breathing intensity in coal dust deposition, with smaller particles penetrating deeper into the respiratory system under higher breathing intensities, while larger particles deposit in the upper airways [6]. Exhalation dynamics have also been shown to influence deposition, as polydisperse particles exhibit varying behavior based on activity levels and size; fine particles (PM2.5) deposit predominantly in pre- and post-bifurcation zones during exhalation, while coarse particles (PM2.5–10) display higher deposition efficiencies under vigorous activity, underscoring the compounded risks in occupational settings [7]. In pediatric studies, CFD analyses of nasal airways following maxillary expansion reveal improved airflow dynamics and particle transport efficiency, as increased nasal volume and reduced resistance facilitate deposition in lower airway regions [8]. Additionally, CFD simulations have been instrumental in evaluating the effectiveness of respiratory masks, with lower porosity masks achieving filtration efficiencies of up to 99% for fine particles (PM2.5) under both laminar and turbulent flow conditions, highlighting their importance in reducing occupational exposure [9]. Furthermore, the integration of Taguchi and response surface methodology (RSM) techniques with CFD simulations has revealed that particle size, flow rate, and drug dosage significantly affect microparticle deposition efficiency, with particle size being the most influential factor, particularly in cases involving asthma patients [10]. These findings collectively underscore the complex interplay of physiological, environmental, and protective factors in determining particle behavior within the respiratory system.

Studying the entire bronchioles geometry computationally is highly challenging and time-intensive. As a result, several references have employed simplified mathematical models of bronchioles airways. These models vary in complexity, ranging from very basic designs, such as the one used in [11] to analyze the transport and deposition of microparticles and nanoparticles (1 to 50 nm) in the mid-bronchial tree during inhalation. A more intricate simplified model was utilized by [12], which incorporated additional airway generations. This approach of progressively increasing the number of airway generations was similarly adopted by [13,14], and [15].

The effects of bronchioles geometry change were examined by [16] using an modified actual bronchioles model. The study revealed significant differences in deposition results between the actual bronchioles model and its simplified version. Other research has concentrated on specific parts of the respiratory system. For example, [17,18] investigated particle deposition in the nasal airway, while [19] utilized various CFD models to study the influence of wall roughness on deposition rates within the nasal passages.

To investigate the flow field and particle deposition in the human upper airway system, encompassing the nasal cavity, nasopharynx, oropharynx, larynx, and trachea, [20,21] broadened the scope of their study and developed a detailed model.

Numerous studies, including [22–27], have concentrated on mouth-throat (MT) and upper tracheobronchial (TB) models. This focus is driven by the critical importance of these regions in drug delivery system research. To advance studies in the tracheobronchial region, [28, 29] introduced the Single Individual Path (SIP) modeling approach. This method simplifies the model and accelerates processing by simulating particle deposition across all generations within a single pathway.

The models employed by [30–37] were derived from patient scans, providing a more realistic foundation for their research. However, the complexity of these realistic models, driven by the precision required and the scope of the study, inherently leads to longer computational times as the complexity increases.

The accuracy of computational solutions is significantly influenced by the computational environment and boundary conditions defined for the simulation. Using Fluent software, [38] solved the Navier–Stokes equations along with Newton's second law of motion, assuming steady, incompressible flow. Particle motion was primarily governed by drag and gravity. A parabolic velocity profile was applied at the inlet, under the assumption of fully developed, laminar flow, with randomly distributed particles at the inlet plane. Similarly, [13] adopted a fully developed (parabolic) velocity at the inlet. In the work by [39], CFD simulations were conducted using Fluent 14.0 to model laminar, steady-state airflow during inhalation. Particle transport was modeled using an Eulerian approach, treating nanoparticles as a homogeneous mixture with air, similar to gas transport, without estimating individual particle trajectories.

[20] employed Fluent 6.3 to solve the governing equations for airflow within the complex geometry of the human upper airway. To investigate particle deposition independent of periodic conditions, the flow was assumed to be steady and laminar. Microparticles released at the nasal inlet were tracked using the Lagrangian approach. In [33], particles were treated as spherical, rigid, and non-rotating, introduced into a Newtonian, time-dependent, incompressible, and laminar flow. Influencing factors included Brownian motion, drag, and gravity.

Using ANSYS CFX (Version 15), [40] solved the 3-D Navier–Stokes equations and modeled airflow in the upper bronchioles airways under both laminar and turbulent flow regimes, employing the Shear Stress Transport $k-\omega$ turbulence model. Drag and gravity were identified as the primary forces acting on particles. OPENFOAM CFD software was utilized by [41] to solve fluid governing equations, incorporating bronchioles motion into the Lagrangian particle simulation. In [42], ANSYS FLUENT 15 was used to analyze particle-fluid interactions, including particle tracking and steady-state, incompressible, three-dimensional flow equations. Turbulent properties were modeled using Reynolds stress, turbulent kinetic energy, and specific dissipation rate ϵ equations. Finally, [28] employed a low Reynolds number $k-\omega$ turbulence model for their simulations, highlighting the impact of turbulence in airflow and particle deposition.

Based on the existing literature, numerous investigations have been conducted on respirable dust bronchioles deposition and CFD simulations of bronchioles airways. However, several gaps remain unaddressed. For instance, the impact of using simplified bronchioles airway models on airflow simulations and dust deposition has not been thoroughly explored. Additionally, there is a lack of comparative studies between experimental results in the bronchiolar region and CFD simulations of coal dust deposition using the same geometric model. The effects of external factors, such as air humidity and dust concentration levels around miners, have also been largely overlooked in previous studies. Furthermore, researchers in the literature commonly use a trap-wall boundary condition to model particle–wall interactions in the bronchioless. However, this approach is not sufficiently accurate as it does not account for the complex phenomena of particle attachment and rebound upon bronchioles wall contact. To address these gaps, the current paper compares experimental results of coal dust deposition with CFD simulations using identical geometric models. Moreover, it examines the differences in coal dust deposition between complex bronchioles airway geometries and simplified models, with the goal of developing empirical corrections. These corrections will enable future studies to use simplified bronchioles airway models while achieving results comparable to those obtained with complex geometries. Additionally, a new model for particle–wall interactions will be introduced to improve accuracy. Finally, the study assesses the effects of air humidity and room dust concentration on measurements and deposition calculations, providing insights into these critical but often neglected factors.

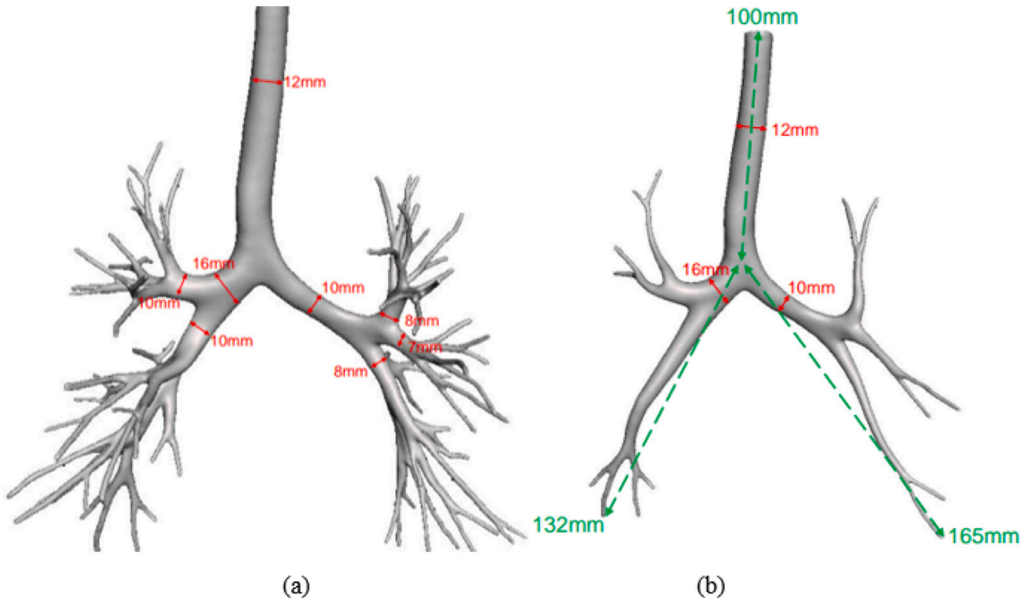

Fig. 1. Bronchioles airways used in the current study. (a) complex bronchioles airways, (b) simplified bronchioles airways.

2. Experimental and computational methods

This section explains the experimental and computational methods employed in this study. The objective is to investigate the deposition of respirable dust within bronchioles models and simulate real-world conditions found in mining environments. A dual approach, combining detailed physical experiments with sophisticated computational simulations, is adopted to provide a comprehensive understanding of dust behavior and its impact on respiratory health for simplified and complex bronchioles model.

2.1. Computational fluid dynamics (CFD) analysis

The Computational Fluid Dynamics (CFD) setup for airflow and particle deposition prediction within the bronchioles models is presented. The CFD analysis process includes obtaining the bronchioles models, meshing, fluid simulation, and particle deposition prediction. All the flow conditions and particles properties were the same as the ones used in the experiments.

Bronchioles models and meshing

The bronchioles models used in the CFD analysis are based on actual human bronchioles geometry. These models were obtained by a medical company through scanning a real person's bronchioles and then the Bronchus and bronchioles converted into a 3D digital model suitable for CFD analysis. The candidate for the scanning is a women in 60's. As the scanned models required some corrections (Cleaning), a separate process was employed to refine the airway models and ensure their accuracy using ANSYS SpaceClaim. A simplified version of the bronchioles model was developed. Simplification was achieved by strategically omitting certain bronchioles from the original geometry. To maintain the anatomical continuity and functional integrity of the airway structure after removal of these bronchioles, the resulting gaps were seamlessly bridged using Spline Surfaces. Fig. 1 illustrates the original and simplified bronchioles models, highlighting the modifications applied to the airway geometry. Table 1 summarizing the key geometric parameters of the complex and simplified bronchioles models, including bounding box dimensions, volume, and surface area.

Upon preparation of the bronchioles models, an intricate meshing process was initiated to establish an effective computational grid essential for the subsequent CFD simulations. In computational fluid dynamics, the mesh serves as the framework within which the equations governing fluid flow and particle interactions are solved. The mesh quality—comprising element size, uniformity, and type—directly influences the accuracy, stability, and convergence of the simulation results.

Table 1
Comparison of geometric features between complex and simplified bronchioles models.

Property	Complex model	Simplified model
Bounding Box Dimensions (mm)	199.9 × 103.2 × 231.0	170.7 × 77.8 × 230.5
Volume (mm^3)	41,625	31,251
Surface Area (mm^2)	28,363	14,788

Table 2
Mesh convergence analysis at location 3: element count, computational time, average velocity, and percent change relative to previous mesh.

Mesh	Elements	Time (s)	Avg velocity (m/s)	Velocity change (%)	Time change (%)
1	774,788	238.6	5.13	–	–
2	1,132,941	369.8	5.22	+1.75%	+55%
3	2,156,817	735.6	5.61	+7.47%	+99%
4	3,907,479	1408.3	5.69	+1.43%	+91%

Given the geometric complexity inherent in bronchioles models, a hybrid mesh combining hexahedral and tetrahedral elements was utilized and generated using Pointwise 14. Hexahedral elements, known for their efficiency in structured mesh regions, enhance calculation speed and accuracy. Tetrahedral elements, on the other hand, offer flexibility in conforming to complex surfaces and intricate details of the bronchioles anatomy. This dual approach allows for an optimized discretization of the space, effectively capturing the critical flow dynamics within the bronchioles, as depicted in Fig. 2.

To ensure the accuracy of the CFD results and validate the chosen mesh configuration, a comprehensive mesh dependency study was conducted. This study evaluated the impact of various mesh densities on simulation outcomes, aiming to balance computational efficiency with precision in the results. The mesh density analysis was performed at three distinct locations within the bronchioles models, as illustrated in Fig. 3. At each location, flow profiles were obtained for four progressively refined meshes.

Table 2 presents the mesh convergence study, showing the effect of mesh refinement on computational time and predicted average

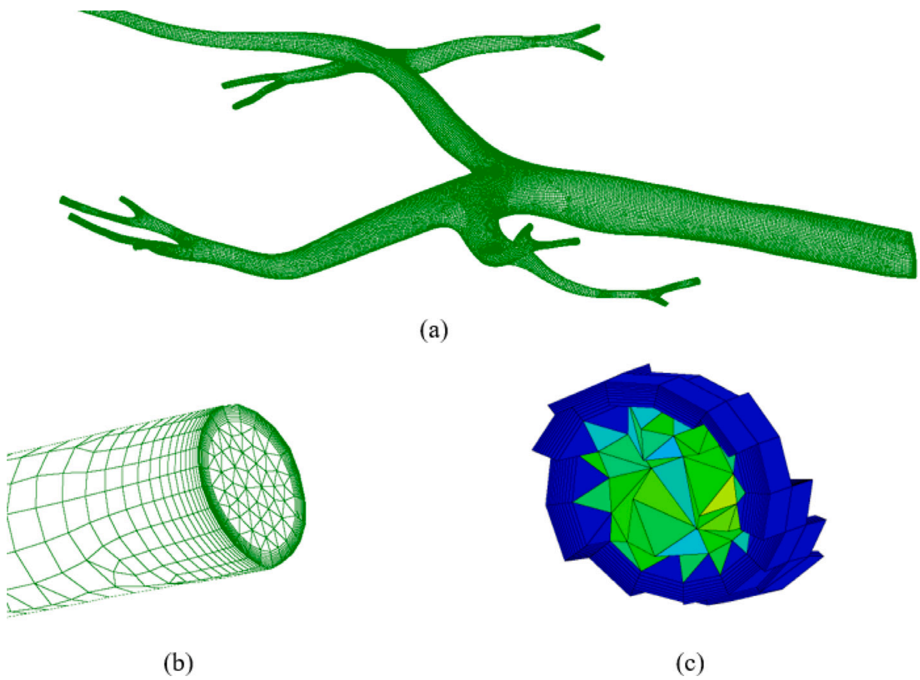

Fig. 2. Illustration of the hybrid hexahedral-tetrahedral mesh employed in the bronchioles models, (a) showcasing the mesh, (b) shows zoomed view of the mesh and (c) shows the mesh structure.

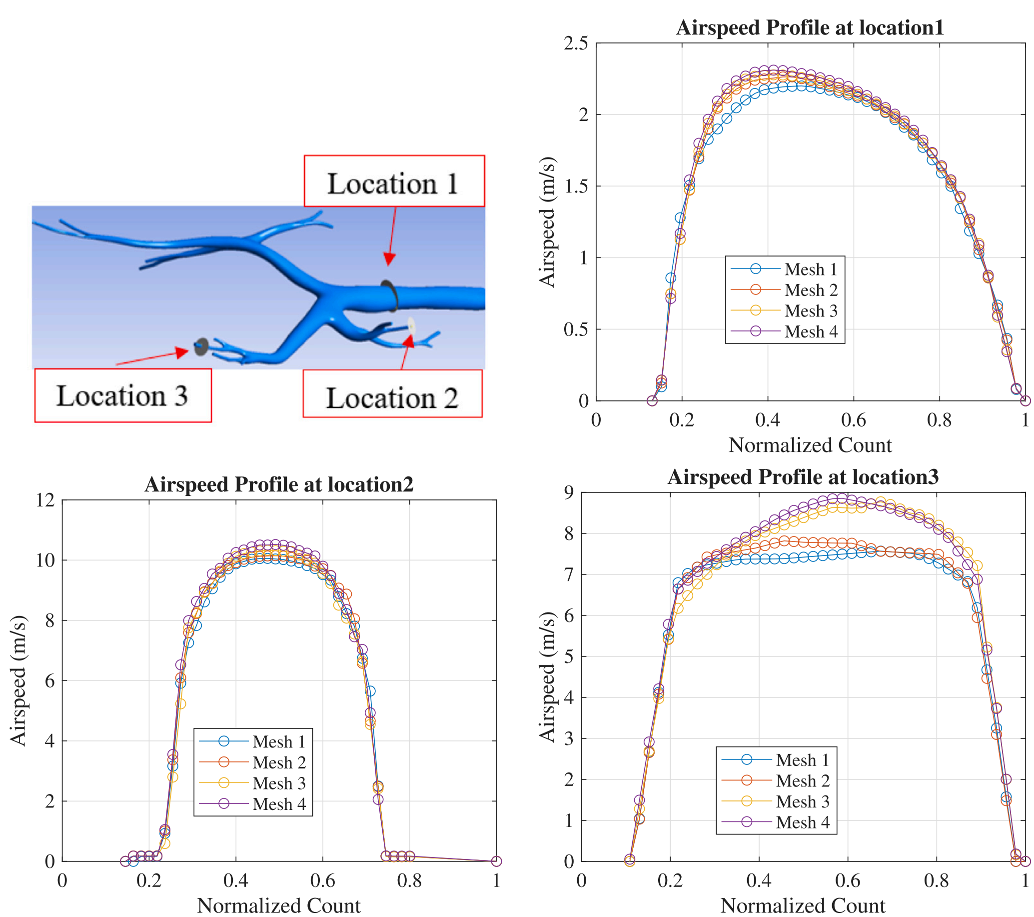

Fig. 3. Evaluation of mesh dependency impacts on simulation accuracy, depicted across three locations within the bronchioles model, utilizing four increasingly refined meshes. Each successive mesh increases by a factor of 1.25.

velocity. The element count increased from approximately 0.77 million to 3.9 million across the four meshes. While average velocity increased with mesh density, the improvement from Mesh 3 to Mesh 4 was marginal (1.43%) compared to the significant increase in computational time per 5000 iterations (91%). This indicates diminishing returns beyond Mesh 3 and suggests that Mesh 3 achieves mesh independence while maintaining a reasonable computational cost.

Consequently, it was determined that the simplified bronchioles model would be configured with approximately 2 million elements (equivalent to Mesh 3), while the more complex model would comprise close to 5 million elements. This configuration ensures a detailed and accurate representation of the bronchioles geometries without compromising computational feasibility.

Probabilistic particle trapping method

A critical aspect of simulations involves the definition of appropriate boundary conditions at the walls, which significantly influence the outcome of particle behavior and deposition. There are several types of wall boundary conditions available, each tailored to model different physical phenomena:

Trap: This boundary condition assumes that all particles impacting the wall are immediately captured and remain adhered. It is the simplest form of interaction and does not account for any rebound or sliding along the wall.

Reflect: Under this condition, particles that collide with the wall are reflected back into the domain. The angle of reflection is typically equal to the angle of incidence, mirroring elastic collision behavior.

Wall Jet: This boundary condition is used to model situations where particles impacting the wall may slide or roll along the surface, influenced by local shear forces. It is particularly useful in scenarios where the tangential components of velocity are significant.

Wall Film: In this more complex scenario, particles that hit the wall form a film or layer, which can flow and undergo further interactions with incoming particles. This condition is useful for simulating spray dynamics where liquid films are formed on surfaces.

In the existing literature, the majority of studies utilize the 'trap' boundary condition when modeling particle–wall interactions. This approach is widely adopted due to its simplicity and the definitive outcomes it provides. However, when comparing simulation results to our experimental findings, notable discrepancies become evident. In our experiments, conducted using dry bronchioles models, coal dust particles exhibited varying behaviors, some particles were trapped upon contact, while others rebounded or slid along the surface. This behavior is influenced by the dry conditions, which differ significantly from the wet environment of real bronchioles. In actual physiological conditions, where the bronchioles surfaces are wet, particles are more likely to adhere due to the cohesive forces facilitated by surface moisture.

These differences underscore the limitations of the 'trap' boundary condition in accurately simulating particle behavior under realistic conditions. While a direct comparison with real, wet bronchioles environments would provide a more accurate validation of simulation models, achieving this is extremely challenging due to the inherent complexities and ethical considerations involved in replicating such scenarios in our experiment.

The probabilistic particle trapping method implemented via a User-Defined Function (UDF) in ANSYS Fluent is designed to simulate the realistic deposition behavior of particles within complex geometries, such as bronchioles airways. This method was inspired by [43] and calculates the probability of particle entrapment upon surface impact, taking into account several critical factors: The particle's impact velocity, angle of impact, diameter (indicative of inertia), and the surface roughness. The overall trapping probability, P_{trap}, is quantified using the following mathematical model:

$$P_{\text{trap}} = \exp\left(-\frac{\alpha}{A_{\text{factor}}}\right)\cdot\exp\left(-\frac{v_{\text{imp}}}{V_{\text{factor}}}\right)\cdot\exp\left(-\frac{d_{\text{p}}}{I_{\text{factor}}}\right)\cdot S_{\text{roughness}}\cdot T_{\text{factor}}$$

In the described model, several parameters are defined to characterize particle interaction and deposition dynamics. The term α represents the impact angle, which is the angle between the particle's trajectory and the surface normal, indicating the approach angle at which a particle strikes the surface. To account for variations in how different angles affect deposition, A_{factor}, referred to as the angle factor, modulates this sensitivity.

The particle's impact velocity is denoted by v_{imp}, which directly influences the kinetic energy at the point of contact with the surface. The velocity factor, V_{factor}, adjusts the effect of this impact velocity on the likelihood of particle trapping, incorporating dynamic conditions into the model.

Particle diameter, represented by d_{p}, encapsulates the inertia of the particle, reflecting its ability to resist changes in motion due to its mass. Associated with the particle diameter, the inertia factor, I_{factor}, quantifies the effect of particle size on trapping efficiency, highlighting size-dependent deposition behaviors.

Surface characteristics are included through $S_{\text{roughness}}$, which quantifies the surface roughness. This factor enhances the likelihood of particle adhesion by providing additional mechanical interlocking opportunities for particles. Additionally, T_{factor}, known as the turbulence factor, accounts for the influence of airflow turbulence on particle paths and their subsequent deposition on the surface, integrating environmental variability into the deposition process.

The computation begins by determining the impact angle α and the velocity v_{imp} from the particle's velocity vector relative to the surface normal vector. The trapping probability P_{trap} is then calculated by exponentiating the negative ratios of these factors to their respective controlling parameters. This probabilistic approach enables a more nuanced simulation of particle behavior, allowing for some particles to be trapped due to their dynamic properties and interactions with the surface, while others rebound. The parameters A_{factor}, V_{factor}, I_{factor}, $S_{\text{roughness}}$, and T_{factor} were meticulously tuned through a trial-and-error process for simplified bronchioles geometry to achieve high alignment with the experimental results. For example, the inertia-related parameter (I_{factor}) was adjusted to implicitly account for the effect of humidity, as observed in the experiments. Higher humidity levels reduced dust deposition, likely due to hygroscopic particle growth, which increases aerodynamic diameter and alters inertial behavior, making particles less likely to adhere to the airway walls. Once optimized, these parameters were consistently applied across all simulation cases and bronchioles models to ensure uniformity and realistic outcomes in the simulations. The parameters used in the probabilistic particle trapping model based on the trial-and-error approach were: The inertia-related parameter $I_{\text{factor}} = 0.1$, the velocity component to $V_{\text{factor}} = 0.5$, the impact angle component to $A_{\text{factor}} = 0.1$, and the surface interaction component to $S_{\text{roughness}} = 0.3$. A normalization term of $T_{\text{factor}} = 1$ was used to scale the trapping probability. This model provides a flexible framework that can be adapted to simulate wet environments by adjusting $S_{\text{roughness}}$, which governs particle adhesion to the wall and reflects increased deposition under moist conditions.

CFD simulation and particle tracking

ANSYS Fluent 19 was employed to conduct a detailed Computational Fluid Dynamics (CFD) and particle tracking simulation using discrete phase simulation (DPM) to study the dynamics of respirable coal dust within a bronchioles model. The simulations utilized a pressure-based solver, configured for transient analysis, crucial for capturing the temporal variations and dynamic interactions between the bronchioles's airflow and particulate phases. The governing equations for the fluid flow, incorporated into this CFD study, are the Navier–Stokes equations for incompressible flow, given by:

$$\nabla \cdot \mathbf{u} = 0 \quad \text{(Continuity Equation)} \tag{1}$$

$$\frac{\partial \mathbf{u}}{\partial t} + (\mathbf{u}\cdot\nabla)\mathbf{u} = -\frac{1}{\rho}\nabla p + \nu\nabla^2\mathbf{u} + \mathbf{f} \quad \text{(Momentum Equation)} \tag{2}$$

where $\mathbf{u}$ represents the velocity field, p the pressure, ρ the fluid density, ν the kinematic viscosity, and $\mathbf{f}$ the body forces per unit mass, which in this case includes gravity. These equations are solved using the Finite Volume Method (FVM) to ensure the accuracy of airflow patterns and particle trajectory simulations within the complex geometries of the bronchioles model.

Turbulence modeling is an integral component of Computational Fluid Dynamics (CFD) that predicts the behavior of fluid flows with chaotic eddies and fluctuations. These models are vital for accurately simulating the complex flow dynamics in environments like human bronchioles airways, where flow patterns significantly influence particle deposition and air quality assessments. For this purpose, the k-omega Shear Stress Transport (SST) model was employed to model the turbulence within the bronchioles airways. This model is particularly effective in managing adverse pressure gradients and flow separations within the complex geometries of the bronchioles. Key enhancements such as Low Reynolds Number (LRN) corrections and curvature corrections were integrated to refine the model's fidelity near wall boundaries and in high-curvature regions, common in anatomically realistic bronchioles models. The governing equations from [44] for the k-omega SST model are:

$$\frac{\partial k}{\partial t} + \mathbf{u} \cdot \nabla k = P_k - \beta^* k\omega + \nabla \cdot \left[(\nu + \sigma_k \frac{\nu_t}{\omega}) \nabla k \right] \tag{3}$$

$$\frac{\partial \omega}{\partial t} + \mathbf{u} \cdot \nabla \omega = \frac{\alpha}{\nu_t} P_k - \beta\omega^2 + \nabla \cdot \left[(\nu + \sigma_\omega \frac{\nu_t}{\omega}) \nabla \omega \right] + 2(1 - F_1) \frac{\sigma_{\omega 2}}{\omega} \frac{\nabla k \cdot \nabla \omega}{\beta^*} \tag{4}$$

where k is the turbulence kinetic energy, ω is the specific dissipation rate, P_k represents the production of turbulence kinetic energy due to mean velocity gradients, and ν_t is the turbulence viscosity. The model constants β^*, σ_k, α, β, and σ_ω are part of the model coefficients, and F_1 is a blending function that transitions between the k-omega and k-epsilon models in the near-wall region. The boundary conditions at the bronchioles inlet as velocity inlet and outlet as pressure outlet.

For the simulation of respirable dust within the bronchioles models, an Eulerian–Lagrangian approach was employed, offering substantial benefits in modeling complex airflow behaviors and particle dynamics. This method is essential for understanding how dust particles deposit on bronchioles surfaces under various respiratory conditions. Such detailed simulation capabilities are critical for assessing health impacts in occupational settings with dust exposure, providing insights into the effectiveness of control strategies and respiratory protection technologies.

The simulation utilized the Discrete Phase Model (DPM) in ANSYS Fluent, with one-way coupling applied due to the low particle volume fraction (less than 10%). In this framework, the airflow field was solved using an Eulerian method, while the trajectories of individual particles were tracked in a Lagrangian manner. This coupling accurately captures the interactions between the dispersed phase (particles) and the continuous phase (air), enabling reliable prediction of particle transport and deposition.

The particle motion was governed by Newton's second law, incorporating both drag and gravitational forces. The general force balance on a particle is expressed as:

$$\frac{d\mathbf{u}_p}{dt} = \frac{18\mu}{\rho_p d_p^2} \cdot \frac{C_D \mathrm{Re}_p}{24} (\mathbf{u} - \mathbf{u}_p) + \mathbf{g} \left(\frac{\rho_p - \rho}{\rho_p} \right) \tag{5}$$

where $\mathbf{u}_p$ is the particle velocity, $\mathbf{u}$ is the fluid velocity, μ is the fluid dynamic viscosity, ρ and ρ_p are the fluid and particle densities, d_p is the particle diameter, and C_D is the drag coefficient based on the particle Reynolds number Re_p. The default DPM implementation in ANSYS Fluent was used [45].

To simulate gravitational settling, the gravitational force acting on each particle was also modeled:

$$F_{\text{gravity}} = m \cdot g \tag{6}$$

where m is the particle mass and g is the gravitational acceleration.

For particle injection and behavior, surface injection was applied at the bronchioles inlet, with the particle velocities matched to the local airflow velocity to reflect realistic inhalation conditions. The Stokes–Cunningham drag law was applied to account for slip effects, especially for submicron coal dust particles in the transitional flow regime:

$$F_d = 3\pi\mu d_p C_c \left(\frac{u_p - u_f}{C_c} \right) \tag{7}$$

where F_d is the drag force, μ is the dynamic viscosity, d_p is the particle diameter, C_c is the Cunningham correction factor, u_p is the particle velocity, and u_f is the fluid velocity.

Stochastic tracking was enabled using a discrete random walk model and random eddy lifetimes to represent the turbulent dispersion of particles.

Solver stability and accuracy were maintained using the SIMPLE algorithm for pressure–velocity coupling, and all numerical schemes were set to second-order to capture the detailed flow structures without compromising computational efficiency.

The Computational Fluid Dynamics (CFD) settings, including the boundary conditions for the fluid dynamics simulations and particle trajectory predictions, are crucial for accurately modeling the behavior of dust within bronchioles models. Fig. 4 illustrates the boundary conditions applied in the simulation. It also shows the locations for velocity profiles (L) and the secondary flow analysis locations (C) which will be used in the results section. Both simplified and complex bronchioles models considered a velocity inlet boundary condition where dust is injected using a Rosin-Rammler distribution to closely mimic the particle size distribution observed in typical respiratory environments. The outlets are configured as pressure outlets allowing for dust escape. The wall boundaries employ a probabilistic trap condition, which reflects the likelihood of particle adhesion upon contact, based on their kinetic properties and the wall's physical characteristics, The summary of the boundary conditions are detailed in Table 3.

The Rosin-Rammler parameters used for dust injection were derived from experimental particle size measurements collected using a laser-based particle sizer during dust injection tests on the physical bronchioles models. As shown in Fig. 5a, particle size distributions were recorded for various mass flow rate samples (S1, S2, S3, and S4) and fitted to the Rosin-Rammler function to represent the observed mass concentration profiles best. The fitting with the Rosin-Rammler function for S3 was performed for illustrative purposes, showing how the samples can be fitted with the Rosin-Rammler function. A pivotal aspect of this analysis involves comparing the experimental data with CFD predictions to validate the accuracy of the simulations. The cumulative number fraction comparison, as depicted in Fig. 5b, shows a close match between the experimental and CFD dust settings. Furthermore, Fig. 5c illustrates the dust injected and escaped during the simulation. The simulation process begins by injecting dust after 0.02 s, monitoring the mass of dust that escapes through the outlet. The difference between the injected and escaped dust mass quantifies the dust deposited inside the bronchioles models. This measurement process, applied consistently across both simplified and complex bronchioles models, provides a robust framework for assessing the efficiency of particle capture by each model type.

Additionally, a time-dependent study was conducted to determine the optimal time steps for the simulation. The study analyzed the escaped mass from the bronchioles models at different time steps, as summarized in Table 4. Results indicate minimal variation in escaped mass between time steps of 0.01 and 0.005 s, leading to the selection of 0.01 s as the standard time step for all further simulations.

2.2. Dust wind tunnel testing

A custom-designed blowing-type wind tunnel shown in Fig. 6, was utilized to replicate underground coal mine conditions, enabling controlled investigations of dust behavior and deposition, particularly

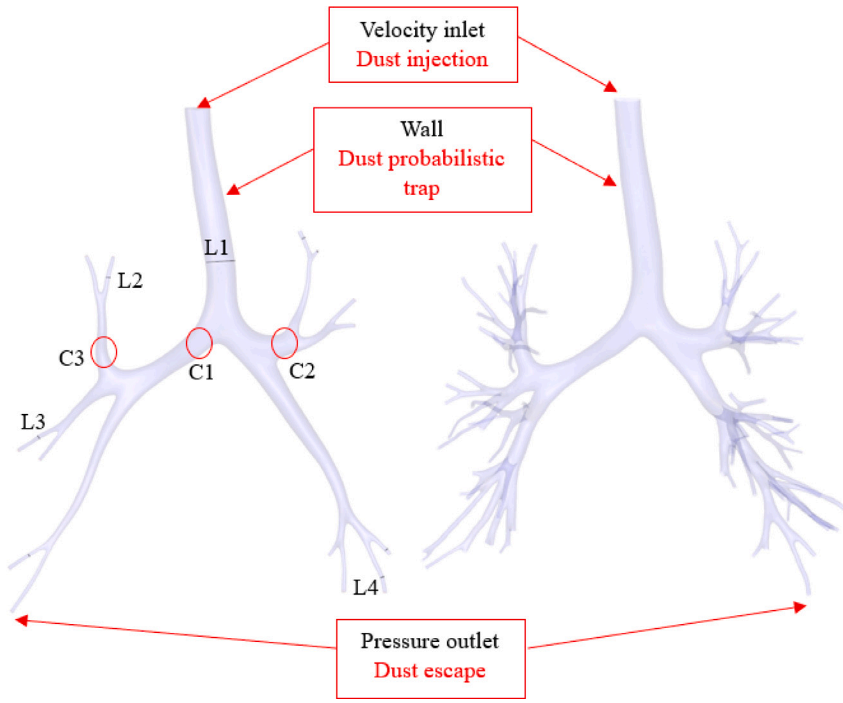

Fig. 4. CFD-DPM simulation boundary conditions for simplified and complex models. It highlights the specific locations designated for cross-flow studies, marked as 'C', and the points for measuring velocity profiles, labeled as 'L'.

Table 3
Summary of CFD simulation boundary conditions.

Boundary	Condition description
Inlet	Velocity inlet: 3.23 m/s (matched to experimental value)
Outlet	Pressure outlet: 0 Pa (atmospheric pressure)
Wall	No-slip condition with probabilistic trap condition
Turbulence model	k–ω SST with standard constants
Discrete Phase Injection	Surface injection at inlet, matched to inlet velocity
Particle Diameter Distribution	Rosin-Rammler; fitted from experimental data
Flow Coupling	One-way coupling (particle volume < 10%)
Numerical Schemes	Second-order for pressure, momentum, turbulence, and DPM
Time Stepping	Transient simulation

Table 4
Time step study showing the escaped dust mass at various intervals.

Time (s)	0.005	0.01	0.02
Escaped Mass	8.72198×10^{-21}	8.62521×10^{-21}	9.11513×10^{-21}

through its integration with an Aerosol bronchioles Deposition Apparatus [46].

This experiment leverages a validated system to examine the deposition patterns of coal dust across two bronchioles models varying in complexity. By conducting a series of controlled experiments, this study not only quantifies coal dust deposition in these models but also elucidates the impact of structural complexities on deposition patterns. Such comparisons are expected to illuminate the key factors influencing dust behavior in human bronchioless, thereby enhancing health and safety strategies in occupational environments, especially within the mining industry.

The bronchioles models were meticulously crafted using resin-based Stereolithography (SLA) 3D printing, chosen for its precision and ability to faithfully replicate the intricate anatomical features of human bronchioless.

Fig. 7a provides a comprehensive view of the overall setup, incorporating the sensor box and an aerosol particle sizer. It also offers a detailed look inside the mannequin used in the experiments, showcasing how the aerosol distribution mechanisms are aligned with the respiratory tract modeling.

The sensor box shown in Fig. 7b ensures that each sensor is isolated from external dust and from each other, optimizing the measurement conditions for precise dust concentration assessment. This isolation is critical to prevent cross-contamination between sensors and to minimize environmental impacts on the measurement results.

Figs. 7c and d illustrate the installation of both the simplified and complex bronchioles models within the wind tunnel used during the experiments. These figures provide a detailed zoomed view of the models, showcasing the tubing and casing integrated into each model to facilitate dust collection post-experiment. For the simplified bronchioles model, a direct tubing method was implemented to streamline the setup. Conversely, the complex model required an alternative approach to accommodate its intricate airway branching, ensuring efficient dust collection.

In this experiment, the SPS30 PM2.5 sensor, designed for air quality applications, was used with the designed sensor box to measure particulate matter with diameters up to 2.5 μm. it is a laser-based optical sensor. The deposition measurement involves quantifying the dust concentration at the bronchioles model's inlet and subtracting the concentration observed at the outlet. This process necessitates simultaneous measurement of dust concentrations, thus requiring the use of two dust sensors.

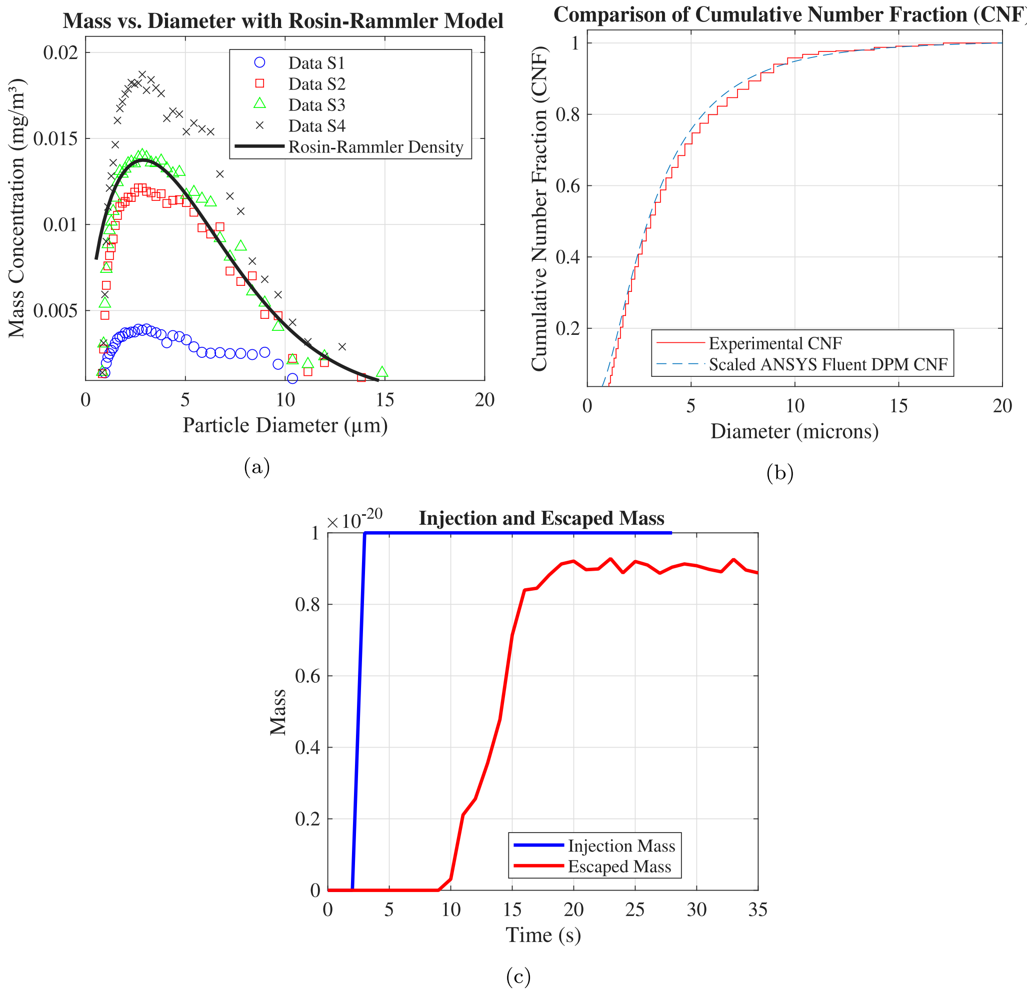

Fig. 5. (a) Fitting of experimental particle size distribution data to the Rosin-Rammler model, (b) Comparison of cumulative number fraction between experimental dust data and CFD predictions, (c) Observation of escaped dust mass from the bronchioles model outlet following dust injection in the CFD-DPM simulation.

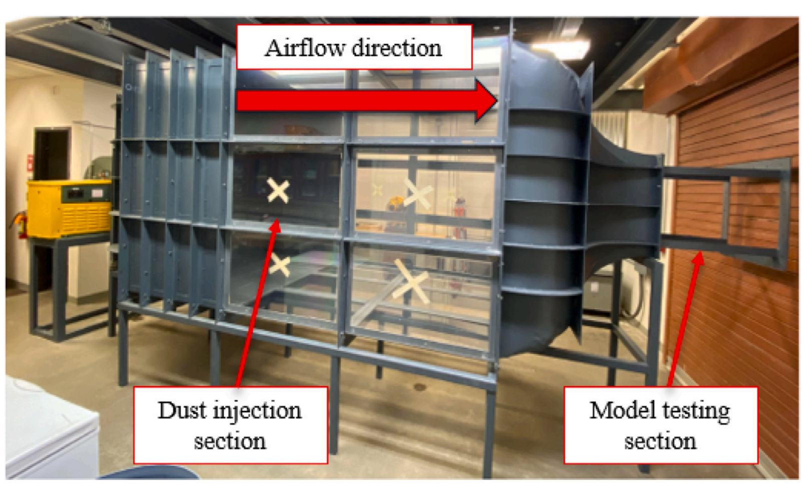

Fig. 6. Dust wind tunnel utilized for experimental assessments.

Experimental setup and measurement protocols

There were three dust sensors used in the experiment. Sensor 1 measures the dust concentration in the wind tunnel while Sensor 2 is dedicated to measuring the dust concentration within the bronchioles model, furthermore Sensor 3 measures the dust concentration exiting the bronchioles. Additionally, an aerosol particle sizer is integrated into the setup to provide detailed particle size distribution data. The vacuum pump plays a critical role in mimicking the inhalation essential for realistic simulation conditions.

Ambient conditions such as air temperature and humidity, along with dust levels in the test section, are continuously monitored using Dust Sensor 1. Each experiment begins by activating the wind tunnel

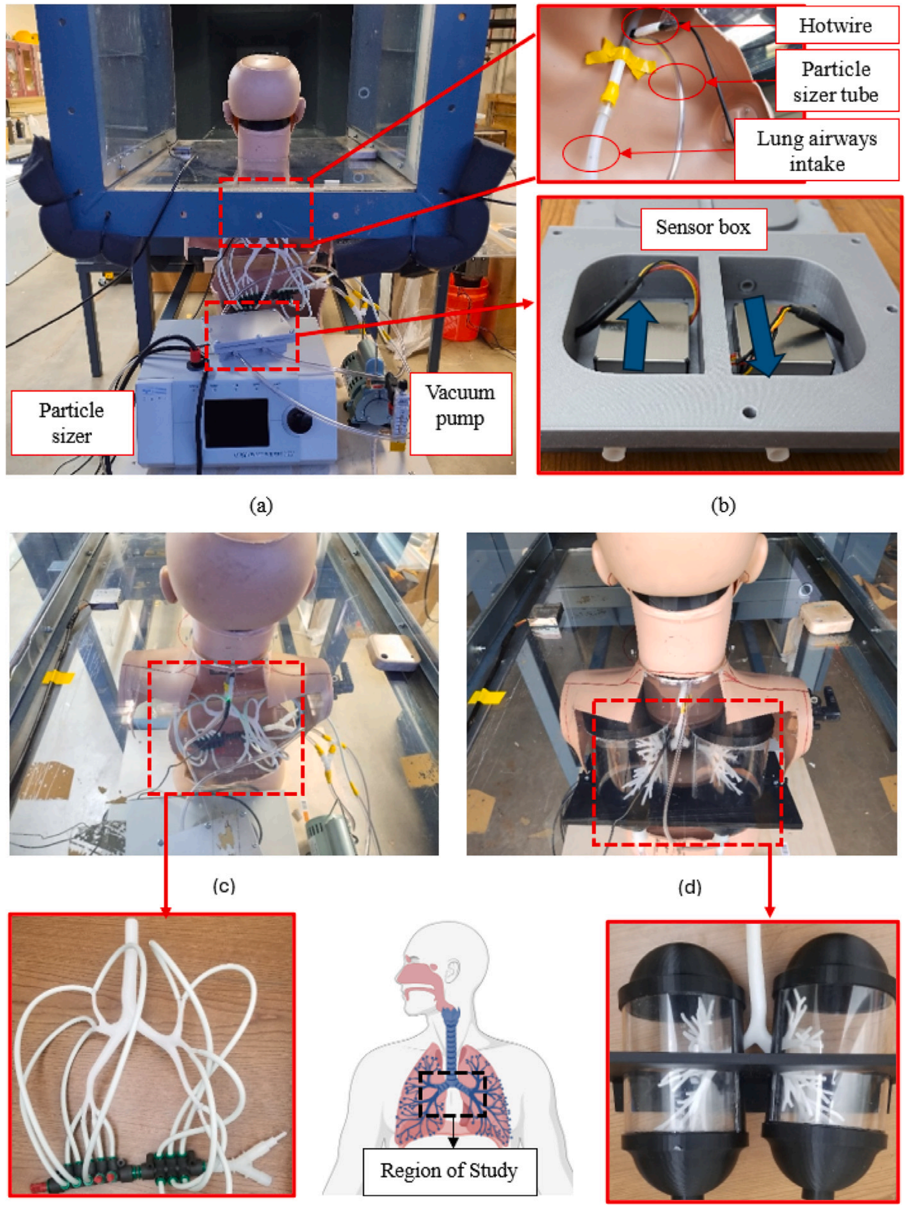

Fig. 7. Experimental setup used with the dust wind tunnel experiment. (a) Overview of the experimental setup featuring a detailed view inside the mannequin, illustrating the integration of various components. (b) Sensor box setup, demonstrating the isolation and airflow optimization critical for accurate dust measurement. (f) Installation of both simplified and complex bronchioles models in the wind tunnel.

to establish a consistent airspeed of 1 m/s, which mirrors the average ventilation speed in underground coal mines. Subsequently, dust is introduced into the wind tunnel test section, and its behavior is monitored by Dust Sensor 1. During this phase, the vacuum pump remains deactivated to prevent any premature movement of dust through the system, as illustrated in Fig. 8(a).

Once the dust concentration stabilizes, the vacuum pump is activated to generate a 3.2 m/s airflow in the bronchioles airways model, corresponding to an inhalation rate of 30 liters per minute. This setup allows dust to pass sequentially through Sensor 2 and then Sensor 3, effectively simulating the inhalation process within the bronchioles model, as depicted in Fig. 8(b). Data collection occurs at a rate of one sample per second over a five-minute duration. To ensure robustness and reproducibility, the experiments are conducted six times for each bronchioles model under varying conditions of humidity and dust concentration.

Following each experimental run, a thorough cleaning process is initiated to prepare the system for subsequent tests. This involves discontinuing the dust generator while keeping both the vacuum pump and wind tunnel operational until all residual particles are cleared from the system, ensuring no cross-contamination occurs between experiments. This cleaning phase is crucial for maintaining the integrity of each test and is visually detailed in Fig. 8(c).

During the experiments, a hot wire anemometer was employed to accurately measure the airflow speed and its fluctuations within the bronchioles model. This tool is crucial for capturing dynamic airflow characteristics, which significantly impact particle transport and deposition patterns. The precise airflow measurements obtained are depicted in Fig. 9a, with a detailed zoomed view provided in Fig. 9b. These results are vital for ensuring consistent boundary conditions in both the experimental setup and the corresponding CFD simulations, facilitating a direct comparison of airflow dynamics under controlled conditions.

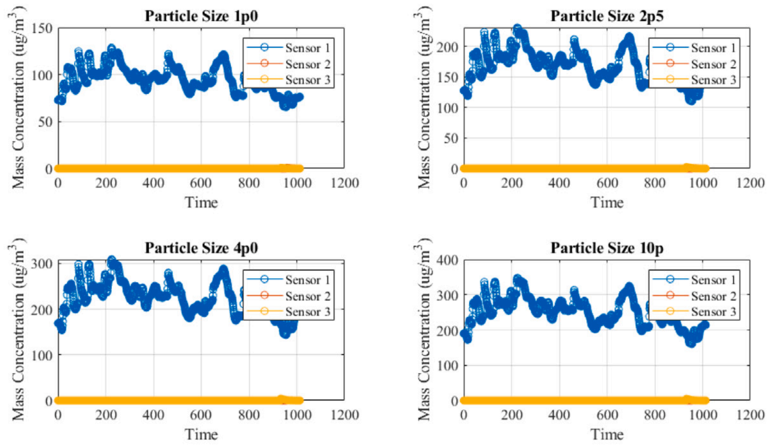

(a) Initial dust monitoring with vacuum pump deactivated.

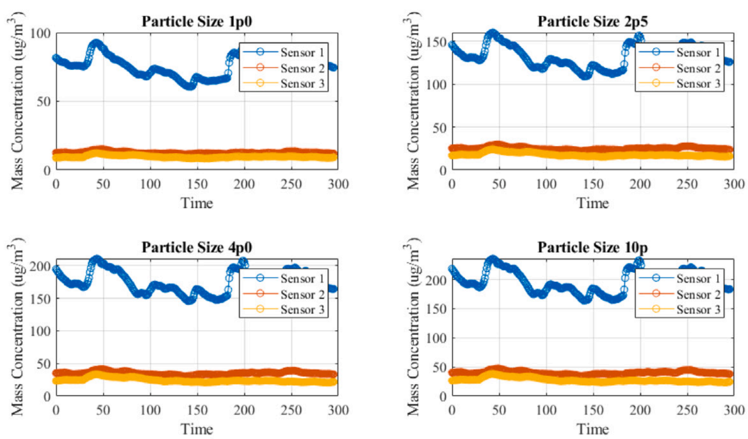

(b) Dust tracking through the bronchioles model with vacuum pump activated.

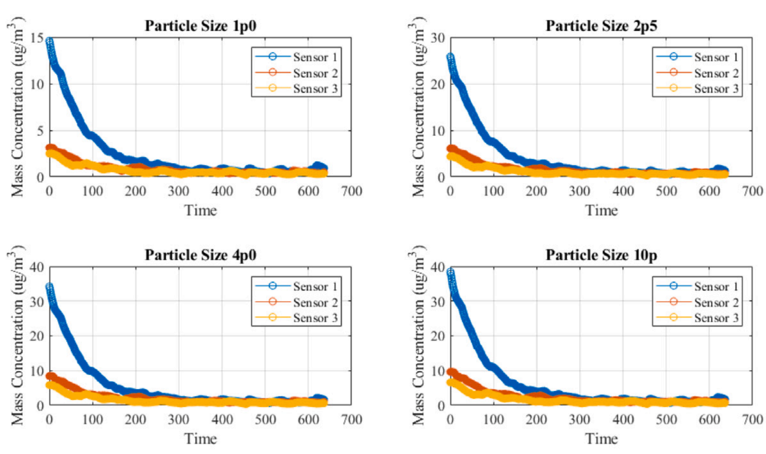

(c) Cleaning process post-experiment to ensure system integrity for subsequent runs.

Fig. 8. Sequential steps in the dust monitoring process: (a) Monitoring initial dust levels, (b) Tracking dust through the bronchioles model, and (c) Post-experiment cleaning.

Furthermore, the particle distribution entering the bronchioles was quantitatively assessed using a particle sizer. This device provided detailed insights into the size distribution of the particulates, which is essential for modeling particle behavior accurately within the bronchioles model.

2.3. Particle imaginary velocity (PIV)

The primary advantages of PIV include its non-intrusive nature and the capability to capture instantaneous velocity measurements across an entire plane, rather than just point measurements as is common with techniques like hot-wire anemometry. These features make PIV

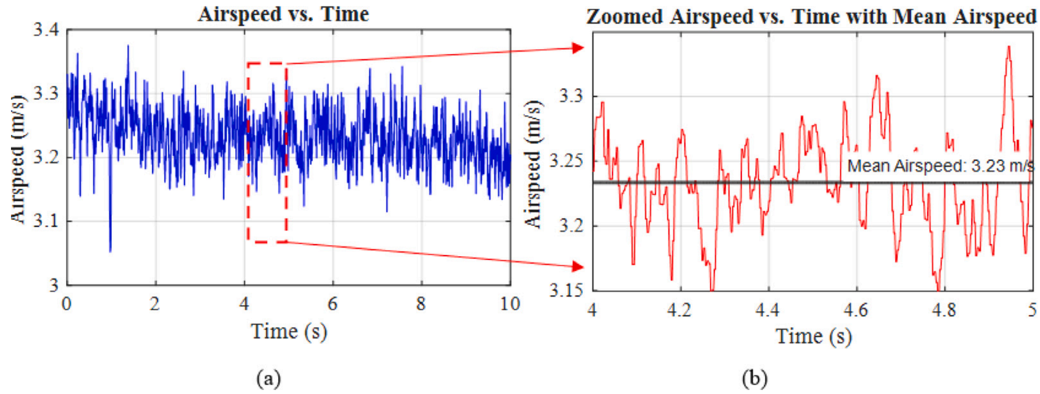

Fig. 9. (a) Measurement of bronchioles inlet airflow speed and fluctuations using a hot wire anemometer. (b) Zoomed view of the airflow measurement highlighting detailed fluctuations.

especially suitable for validating Computational Fluid Dynamics (CFD) simulations, as it facilitates direct comparison between experimental and simulated velocity fields. To validate the CFD simulation results for the airflow inside the bronchioles, a PIV experiment was conducted using fabricated silicone models. These models were intricately designed to closely replicate the complex geometry of the human bronchioles. They were carefully constructed to ensure accuracy and reliability in the experimental results. Since the models are not fully transparent, they were submerged in a water-glycerin mix to match the refractive index of the model walls and minimize the laser sheet reflecting off the model walls. The ratio of water to glycerin was 4:6.

3. Bronchioles model geometry simplification assessment

The assessment of the simplification of the geometry of bronchioles models is presented in this section. The primary objective is to evaluate the viability of using simplified bronchioles models in both physical experiments and CFD simulations. By comparing the outcomes obtained from detailed complex models with those from their simplified counterparts, it is aimed to establish criteria and thresholds for simplification that retain essential geometrical features necessary for reliable predictions.

3.1. Comparison of CFD and PIV results

The operational setup of the system, with the laser actively illuminating the bronchioles model, is captured in Fig. 10. This figure compares the velocity vectors and contours obtained from both Particle Image Velocimetry (PIV) and Computational Fluid Dynamics (CFD) analyses. One of the main challenges encountered during PIV imaging was the presence of optical shadows caused by the airway walls and branching geometry. To mitigate this, the model was carefully rotated to minimize shadowed regions and maximize optical access. As a result, the velocity field was successfully captured in selected cross-sectional planes with minimal obstruction. This alignment is demonstrated by the flow profiles in the same figure, where the PIV fluid speed profiles, marked by blue circles, closely align with the CFD predictions depicted by the red curve. Despite the limited optical access, the obtained data was sufficient.

3.2. Assessment of geometry simplification on dust deposition in bronchioles models: Experimental and computational analysis

This section explores how simplifying the geometry of bronchioles models affects dust deposition. experiments and Computational Fluid Dynamics (CFD) simulations were conducted under identical conditions to ensure reliable comparisons. This approach helps us understand the impact of model simplifications on accurately predicting dust behaviors within the bronchioles.

Table 5
Dust deposition in the simplified bronchioles model across different humidity levels.

Humidity (%)	PM1.0 (%)	PM2.5 (%)	PM4.0 (%)	PM10 (%)	Outside PM1.0 (μg/m^3)
17.24	23.78	29.07	30.78	31.33	81
12	29.37	36.85	39.35	40.15	78

Table 6
Dust deposition in the complex bronchioles model across different humidity levels.

Humidity (%)	PM1.0 (%)	PM2.5 (%)	PM4.0 (%)	PM10 (%)	Outside PM1.0 (μg/m^3)
21.76	61.20	64.31	65.47	65.86	88
29.28	22.84	29.08	31.39	32.15	89

Table 7
Dust deposition in the complex bronchioles model at varying dust concentration levels.

Outside PM1.0	PM1.0 (%)	PM2.5 (%)	PM4.0 (%)	PM10 (%)	Humidity (%)
88.76	22.84	29.08	31.39	32.15	29.28
181.01	44.75	44.96	45.04	45.06	28.5

The experimental results were obtained under varying humidity levels and dust concentrations to ensure a comprehensive evaluation of the environmental effects on the deposition. Identical conditions were maintained across both the simplified and complex bronchioles models to facilitate a direct comparison. In all scenarios, the complex model exhibited a higher dust deposition rate than the simplified model. Dust deposition was quantitatively assessed using the formula: $(1 - \frac{dust\_mass\_out}{dust\_mass\_in})$, which was consistently applied in both experimental measurements and CFD simulations.

Significant variations in dust deposition were observed as a function of humidity and dust concentration. These parameters were shown to critically influence coal dust deposition rates, as detailed in the following tables:

As observed, changes in humidity influenced the dust deposition percentages significantly. Similar patterns were noted in the complex bronchioles model.

The experimental results presented in Tables 5, 6, and 7 elucidate the significant role that humidity levels and dust concentrations play in dust deposition within bronchioles models. Across all conditions, the complex bronchioles model consistently showed higher dust deposition rates compared to the simplified model. This can be attributed to the complex model's ability to mimic the intricate structure of human airways, which enhances particle capture through various mechanisms such as impaction and diffusion.

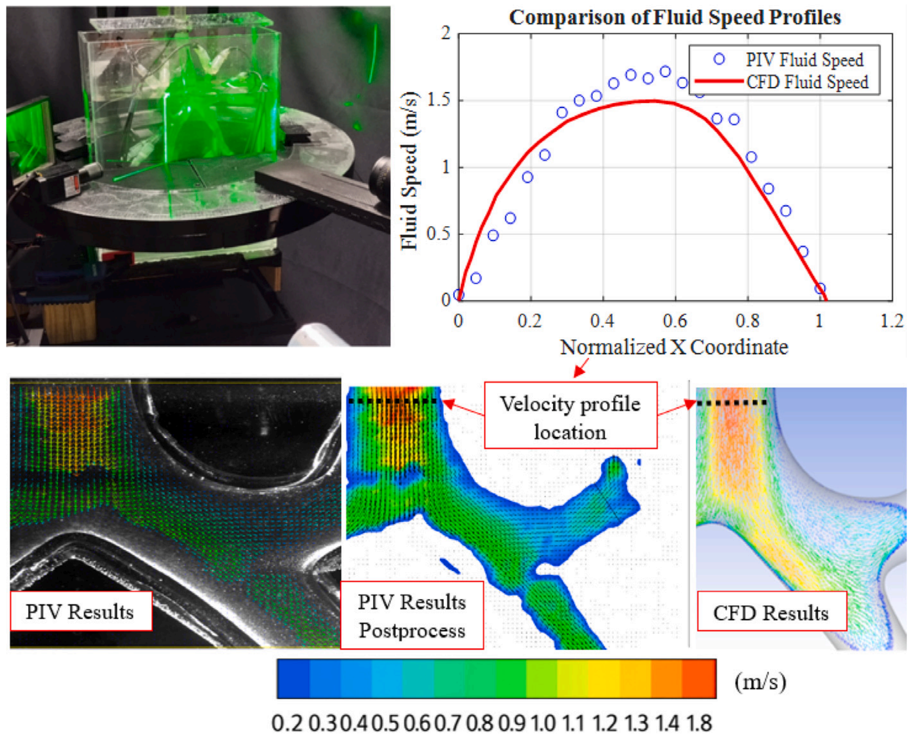

Fig. 10. PIV setup during operation, showcasing the active measurement environment. Adjacent to this, CFD velocity vectors and a comparative analysis of velocity profiles with PIV results are presented, illustrating the correlation and discrepancies between the experimental data and computational predictions.

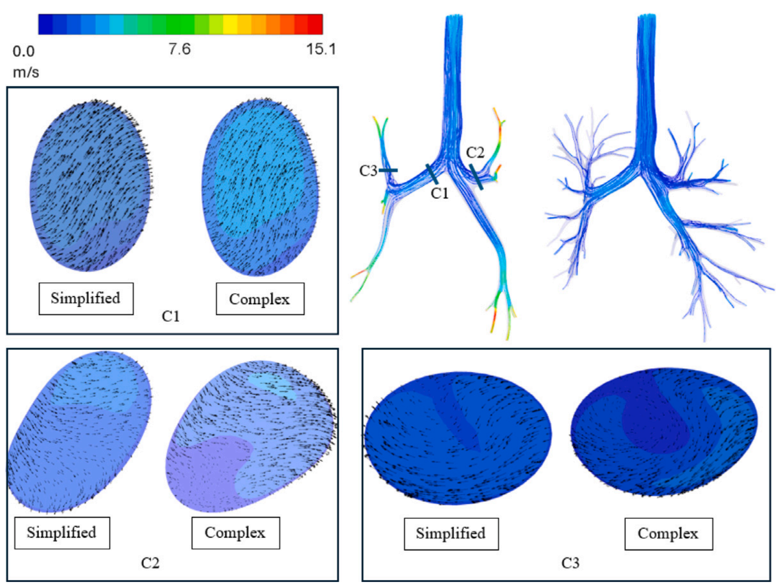

Fig. 11. Streamlines comparing airflow in simplified and complex bronchioles models, highlighting Secondary flow results in different locations.

In Table 5, variations in humidity were observed to influence the deposition rates, with lower humidity generally increasing deposition efficiency. Similar trends were noted in Table 6, where the complex model also demonstrated increased deposition with decreasing humidity, albeit to a different extent due to its geometric intricacies.

Table 7 further highlights how changes in dust concentration levels can impact deposition percentages. Particularly, higher concentrations led to significantly increased deposition rates, suggesting saturation effects and possibly enhanced agglomeration and settling within the complex bronchioles model. This observation underscores the importance of considering particle–particle interactions and airflow dynamics within detailed bronchioles geometries.

Collectively, these findings reinforce the necessity of integrating realistic geometric and environmental variables in both physical and computational models.

To elucidate the influence of bronchioles model geometry on particle deposition, it is essential to first consider the results from CFD. The airflow behavior inside the bronchioles models, illustrated in Fig. 11, reveals critical insights into how airspeed variations and geometric complexities affect coal dust deposition. While the larger diameter sections of both bronchioles models show similar air velocities, significant differences emerge in the smaller diameters and outlet regions. In the complex model, airspeed decreases as it approaches the outlet, whereas

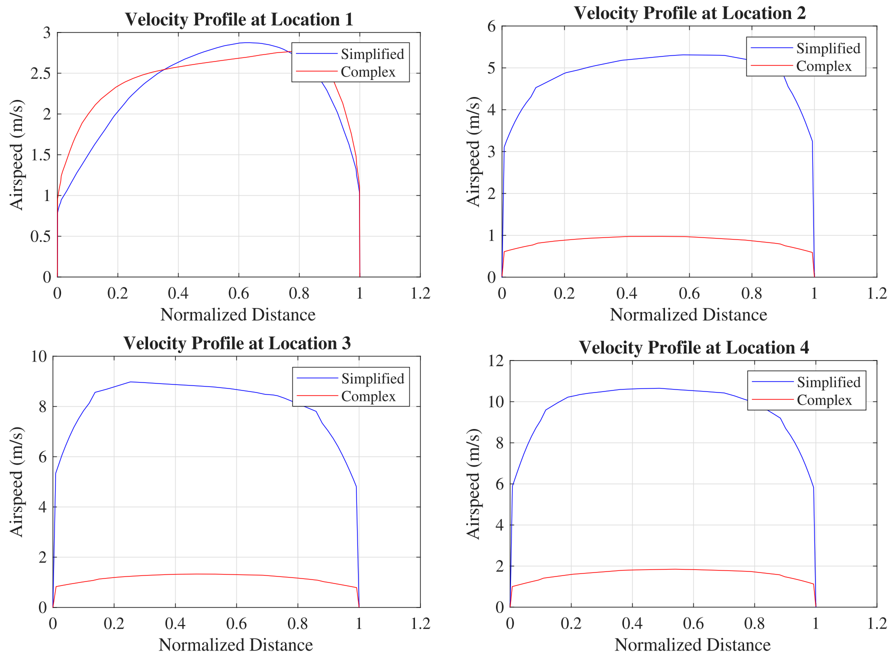

Fig. 12. Velocity profiles within the bronchioles models at different 'L' locations, illustrating distinct patterns significantly influenced by the geometrical configurations.

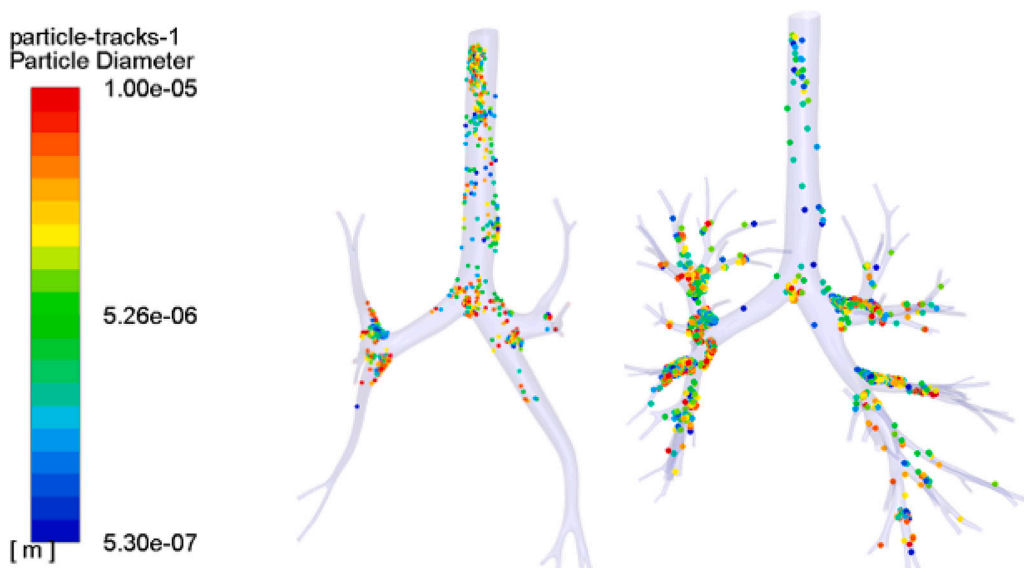

Fig. 13. Comparative visualization of coal dust deposition in simplified and complex bronchioles models, where contour colors highlight the particle diameters.

in the simplified model, the opposite trend is observed—a logical outcome given the reduction in outlet area necessitating increased airspeed to conserve mass.

The secondary flow results in the same figure further supports of these findings by showing the secondary flow patterns, which tend to push particles towards the walls, thereby increasing the likelihood of trapping. This mechanism is particularly pronounced in regions where the airflow undergoes significant directional changes.

Velocity profiles at various points within the bronchioles models, as shown in Fig. 12, corroborate these observations, with the complex model demonstrating a consistent reduction in velocities towards the outlets compared to the simplified model. The deposition patterns, illustrated in Fig. 13, show general similarities between the two models, except at outlet branches where increased airspeed significantly reduces particle trapping due to higher particle momentum.

The comparison between CFD and experimental results, detailed in Table 8, highlights some discrepancies attributable to several factors. While CFD used a spherical dust particles, the actual particle shape in the experiments was more complex. Additionally, inherent errors in fluid simulation and particle tracking contribute to these differences. Despite these, the ratio of increase in dust deposition from the simplified to complex models is consistent with experimental observations, suggesting a corrective factor could be applied for more accurate predictions.

The ratio of the increase in dust deposition between the simplified and complex bronchioles models is approximately 1.5 in the CFD simulations and 1.68 in the experimental observations. This discrepancy can be adjusted with a correction factor of $0.78 \times \left(\frac{\text{Surface area of complex bronchioles}}{\text{Surface area of simplified bronchioles}}\right)$. This correction factor allows for a more accurate calculation of actual dust deposition in the models.

Table 8
Comparison of dust deposition results between CFD and experimental observations.

Model	CFD (%)	Experiment (%)	Difference
Simplified	24	19	5
Complex	36	32	4
Ratio	1.5	1.684210526	–

While the simplified bronchioles model remains a viable option for studying dust deposition mechanisms in areas where airspeed does not significantly change, it may not provide accurate results in regions with high airspeed variability, such as outlets and narrow passages. In studies focusing on these critical areas, it is advisable to adjust the airspeed at the outlet by multiplying it by $0.1\times(\frac{\text{Surface area of complex bronchioles}}{\text{Surface area of simplified bronchioles}})$ to better match the conditions observed in more complex geometries. This adjustment helps in refining the simulation settings to more accurately reflect the behavior observed in complex bronchioles models.

4. Conclusions

The comparative analysis of Computational Fluid Dynamics (CFD) results with data from the Mobile Aerosol bronchioles Deposition Apparatus experiments has been instrumental in advancing our understanding of particle deposition mechanics within bronchioles models. This rigorous comparison not only served to validate our computational models but also illuminated how geometrical simplifications affect particle deposition outcomes. Notably, the complex bronchioles model consistently demonstrated higher particle retention compared to the simplified model. This significant finding underscores the importance of detailed geometric representation in respiratory studies, particularly when aiming to capture the nuanced behaviors of particle interactions within the bronchioles's intricate structures.

The detailed architectural features of the complex bronchioles model allowed for more interaction sites for particles, which likely contributed to its increased retention capacity. These sites, characterized by structural nooks and crannies, provide additional surfaces for particle capture through mechanisms such as impaction and diffusion. This enhanced retention is critical in studies focusing on health impacts where understanding exact deposition locations within the bronchioles can inform targeted therapeutic and preventive strategies.

Moreover, the integration of bronchioles models findings into the CFD simulations enabled targeted adjustments to the models, particularly concerning particle shape and behavioral dynamics. Discrepancies noted between the empirical data and initial simulation outputs led to a targeted recalibration of particle dynamics within the simulations to ensure closer alignment with observed experimental behavior. Specifically, the parameters in the probabilistic particle trapping model, including the inertia factor (I_{factor}), velocity factor (V_{factor}), angle factor (A_{factor}), and surface roughness ($S_{\text{roughness}}$), were tuned through a trial-and-error process to reflect the deposition behavior observed under experimental conditions, including the effects of humidity and wall interaction. In addition, the particle drag behavior was refined by switching to the Stokes–Cunningham drag law to more accurately capture submicron dust behavior. The particle size distribution used in the CFD was also recalibrated by fitting experimental data to a Rosin–Rammler distribution. These refinements improved the accuracy of particle transport and deposition prediction while maintaining computational efficiency.

This iterative process of validation and refinement is central to maintaining the scientific rigor and applicability of our models to real-world scenarios. By continuously updating the simulation parameters based on empirical data, our models not only adhere more closely to the physical realities they aim to replicate but also become more robust tools for predicting particle behavior under various respiratory conditions. This ongoing refinement process enhances the predictive power of our simulations, making them invaluable tools for both research and clinical applications.

Ultimately, the insights gained from comparing CFD simulations with bronchioles models data contribute significantly to the field of respiratory health. They enable researchers and clinicians to better predict where and how particles deposit in the bronchioless, which is crucial for understanding the etiology of respiratory diseases and designing effective interventions. The knowledge derived from these comparative analyses helps bridge the gap between theoretical research and practical, clinical applications, paving the way for advancements in respiratory health diagnostics and treatment.

CRediT authorship contribution statement

Ahmed Aboelezz: Writing – original draft, Visualization, Validation, Methodology, Investigation, Conceptualization. **Wei-Chung Su:** Methodology. **Mohammad Rezaee:** Resources. **Pedram Roghanchi:** Resources, Methodology, Funding acquisition.

Declaration of competing interest

The authors declare that they have no known competing financial interests or personal relationships that could have appeared to influence the work reported in this paper.

Acknowledgment

This research was funded by National Institute for Occupational Safety and Health (NIOSH), grant numbers #75D30119C06390 and #75D30121C12182. The views, opinions, and recommendations expressed here are solely those of the authors and do not necessarily reflect the views of NIOSH. Mention of trade names, commercial products, or organizations does not imply endorsement by the authors or the funding organization.

Data availability

Data will be made available on request.

References

[1] NIOSH coal workers health surveillance program data query system, 2020, https://webappa.cdc.gov/ords/cwhsp-database.html. (Accessed: 2024-06-05).

[2] A. Tsuda, F.S. Henry, J.P. Butler, Particle transport and deposition: basic physics of particle kinetics, Compr. Physiol. 3 (4) (2013) 1437.

[3] E. Madureira, A. Aboelezz, W.-C. Su, P. Roghanchi, From dust to disease: A review of respirable coal mine dust lung deposition and advances in CFD modeling, Minerals 13 (2023) 1311, http://dx.doi.org/10.3390/min13101311.

[4] Y. Cheng, H. Yu, S. Xie, J. Zhao, Y. Ye, Study on the coal dust deposition fraction and site in the upper respiratory tract under different particle sizes and labor intensities, Sci. Total Environ. 868 (2023) 161617, http://dx.doi.org/10.1016/j.scitotenv.2023.161617.

[5] M.M. Rahman, M. Zhao, M.S. Islam, K. Dong, S.C. Saha, Aging effects on airflow distribution and micron-particle transport and deposition in a human lung using CFD-DPM approach, Adv. Powder Technol. 32 (2021) 3506–3516, http://dx.doi.org/10.1016/j.apt.2021.08.003.

[6] H. Peng, A. Tang, W. Nie, Y. Zhang, L. Guo, X. Zhang, J. Li, Multifaceted analysis of the diffusion and deposition patterns of sub-10-μm coal dust particles in the respiratory tract, Process. Saf. Environ. Prot. 190 (2024) 298–313, http://dx.doi.org/10.1016/j.psep.2024.08.003.

[7] M.F. Mehmood, A. Munir, U. Farooq, H.H. Riaz, M. Zhao, M.S. Islam, Breath of impact: Unveiling the dynamics of exhalation-driven deposition of polydisperse particles in lung across varied physical activities, Powder Technol. 448 (2024) 120283, http://dx.doi.org/10.1016/j.powtec.2024.120283.

[8] J.V. Corda, J. Emmanuel, S. Nambiar, P. K, M. Zuber, Airflow patterns and particle deposition in a pediatric nasal upper airway following a rapid maxillary expansion: Computational fluid dynamics study, Cogent Eng. 10 (2023) 2158614, http://dx.doi.org/10.1080/23311916.2022.2158614.

[9] A.A. Tadi, D.J. Jasim, A. Alizadeh, N. Nasajpour-Esfahani, M. Shamsborhan, M. Hekmatifar, Investigating the effect of the absence and presence of a mask with different porosities on the absorption of particulate matter by the human respiratory system using computational fluid dynamics, Ain Shams Eng. J. 15 (2024) 102506, http://dx.doi.org/10.1016/j.asej.2023.102506.
[10] W.-H. Chen, C.-M. Chang, J.K. Mutuku, S.S. Lam, W.-J. Lee, Analysis of microparticle deposition in the human lung by Taguchi method and response surface methodology, Environ. Res. 197 (2021) 110975, http://dx.doi.org/10.1016/j.envres.2021.110975.
[11] M.C. Piglione, D. Fontana, M. Vanni, Simulation of particle deposition in human central airways, Eur. J. Mech. B Fluids 31 (2012) 91–101.
[12] X. Chen, W. Zhong, X. Zhou, B. Jin, B. Sun, CFD–DEM simulation of particle transport and deposition in pulmonary airway, Powder Technol. 228 (2012) 309–318.
[13] Y. Feng, C. Kleinstreuer, Micron-particle transport, interactions and deposition in triple lung-airway bifurcations using a novel modeling approach, J. Aerosol Sci. 71 (2014) 1–15.
[14] M.S. Islam, S.C. Saha, T. Gemci, I.A. Yang, E. Sauret, Z. Ristovski, Y. Gu, Euler-Lagrange prediction of diesel-exhaust polydisperse particle transport and deposition in lung: Anatomy and turbulence effects, Sci. Rep. 9 (1) (2019) 1–16.
[15] X. Chen, Y. Feng, W. Zhong, B. Sun, F. Tao, Numerical investigation of particle deposition in a triple bifurcation airway due to gravitational sedimentation and inertial impaction, Powder Technol. 323 (2018) 284–293.
[16] Y.H. Kim, Z.B. Tong, H.K. Chan, R.Y. Yang, CFD modelling of air and particle flows in different airway models, J. Aerosol Sci. 134 (2019) 14–28.
[17] N. Gao, J. Niu, Q. He, T. Zhu, J. Wu, Using RANS turbulence models and Lagrangian approach to predict particle deposition in turbulent channel flows, Build. Environ. 48 (2012) 206–214.
[18] A.R. Lambert, P.T. O'shaughnessy, M.H. Tawhai, E.A. Hoffman, C.-L. Lin, Regional deposition of particles in an image-based airway model: large-eddy simulation and left-right lung ventilation asymmetry, Aerosol Sci. Technol. 45 (1) (2011) 11–25.
[19] J.D. Schroeter, G.J. Garcia, J.S. Kimbell, Effects of surface smoothness on inertial particle deposition in human nasal models, J. Aerosol Sci. 42 (1) (2011) 52–63.
[20] P.F. Ghalati, E. Keshavarzian, O. Abouali, A. Faramarzi, J. Tu, A. Shakibafard, Numerical analysis of micro-and nano-particle deposition in a realistic human upper airway, Comput. Biol. Med. 42 (1) (2012) 39–49.
[21] J. Xi, X. Si, J.W. Kim, A. Berlinski, Simulation of airflow and aerosol deposition in the nasal cavity of a 5-year-old child, J. Aerosol Sci. 42 (3) (2011) 156–173.
[22] M. Hindle, P. Longest, Evaluation of enhanced condensational growth (ECG) for controlled respiratory drug delivery in a mouth-throat and upper tracheobronchial model, Pharm. Res. 27 (9) (2010) 1800–1811.
[23] P.G. Koullapis, S.C. Kassinos, M.P. Bivolarova, A.K. Melikov, Particle deposition in a realistic geometry of the human conducting airways: Effects of inlet velocity profile, inhalation flowrate and electrostatic charge, J. Biomech. 49 (11) (2016) 2201–2212.
[24] P. Longest, G. Tian, R.L. Walenga, M. Hindle, Comparing MDI and DPI aerosol deposition using in vitro experiments and a new stochastic individual path (SIP) model of the conducting airways, Pharm. Res. 29 (6) (2012) 1670–1688.
[25] Z. Zhang, C. Kleinstreuer, Laminar-to-turbulent fluid–nanoparticle dynamics simulations: Model comparisons and nanoparticle-deposition applications, Int. J. Numer. Methods Biomed. Eng. 27 (12) (2011) 1930–1950.
[26] M. Awadalla, S. Miyawaki, M.H. Abou Alaiwa, R.J. Adam, D.C. Bouzek, A.S. Michalski, M.K. Fuld, G.R. Graff, S.E. Stephenson, R.D. Szczesniak, et al., Early airway structural changes in cystic fibrosis pigs as a determinant of particle distribution and deposition, Ann. Biomed. Eng. 42 (4) (2014) 915–927.
[27] Z. Zhang, C. Kleinstreuer, S. Hyun, Size-change and deposition of conventional and composite cigarette smoke particles during inhalation in a subject-specific airway model, J. Aerosol Sci. 46 (2012) 34–52.
[28] G. Tian, P.W. Longest, G. Su, R.L. Walenga, M. Hindle, Development of a stochastic individual path (SIP) model for predicting the tracheobronchial deposition of pharmaceutical aerosols: Effects of transient inhalation and sampling the airways, J. Aerosol Sci. 42 (11) (2011) 781–799.
[29] P.W. Longest, G. Tian, N. Khajeh-Hosseini-Dalasm, M. Hindle, Validating whole-airway CFD predictions of DPI aerosol deposition at multiple flow rates, J. Aerosol Med. Pulm. Drug Deliv. 29 (6) (2016) 461–481.
[30] A.V. Kolanjiyil, C. Kleinstreuer, Computationally efficient analysis of particle transport and deposition in a human whole-lung-airway model. Part I: Theory and model validation, Comput. Biol. Med. 79 (2016) 193–204.
[31] K. Kadota, A. Imanaka, M. Shimazaki, T. Takemiya, K. Kubo, H. Uchiyama, Y. Tozuka, Effects of inhalation procedure on particle behavior and deposition in the airways analyzed by numerical simulation, J. Taiwan Inst. Chem. Eng. 90 (2018) 44–50.
[32] A.V. Kolanjiyil, C. Kleinstreuer, Computational analysis of aerosol-dynamics in a human whole-lung airway model, J. Aerosol Sci. 114 (2017) 301–316.
[33] P. Koullapis, F. Stylianou, J. Sznitman, B. Olsson, S. Kassinos, Towards whole-lung simulations of aerosol deposition: A model of the deep lung, J. Aerosol Sci. 144 (2020) 105541.
[34] K. Poorbahrami, J.M. Oakes, Regional flow and deposition variability in adult female lungs: A numerical simulation pilot study, Clin. Biomech. 66 (2019) 40–49.
[35] M.S. Islam, S.C. Saha, E. Sauret, T. Gemci, I.A. Yang, Y. Gu, Ultrafine particle transport and deposition in a large scale 17-generation lung model, J. Biomech. 64 (2017) 16–25.
[36] M.S. Islam, S.C. Saha, E. Sauret, T. Gemci, Y. Gu, Pulmonary aerosol transport and deposition analysis in upper 17 generations of the human respiratory tract, J. Aerosol Sci. 108 (2017) 29–43.
[37] A. Lintermann, W. Schr"oder, Simulation of aerosol particle deposition in the upper human tracheobronchial tract, Eur. J. Mech. B Fluids 63 (2017) 73–89.
[38] X. Chen, W. Zhong, J. Tom, C. Kleinstreuer, Y. Feng, X. He, Experimental-computational study of fibrous particle transport and deposition in a bifurcating lung model, Particuology 28 (2016) 102–113.
[39] G.J. Garcia, J.D. Schroeter, J.S. Kimbell, Olfactory deposition of inhaled nanoparticles in humans, Inhal. Toxicol. 27 (8) (2015) 394–403.
[40] A.V. Kolanjiyil, C. Kleinstreuer, R.T. Sadikot, Computationally efficient analysis of particle transport and deposition in a human whole-lung-airway model. Part II: Dry powder inhaler application, Comput. Biol. Med. 84 (2017) 247–253.
[41] R. Mead-Hunter, A.J. King, A.N. Larcombe, B.J. Mullins, The influence of moving walls on respiratory aerosol deposition modelling, J. Aerosol Sci. 64 (2013) 48–59.
[42] O. Pourmehran, M. Rahimi-Gorji, M. Gorji-Bandpy, T. Gorji, Simulation of magnetic drug targeting through tracheobronchial airways in the presence of an external non-uniform magnetic field using Lagrangian magnetic particle tracking, J. Magn. Magn. Mater. 393 (2015) 380–393.
[43] H. Yan, N. Vosswinkel, S. Ebbert, G.L. Kouyi, R. Mohn, M. Uhl, J.-L. Bertrand-Krajewski, Numerical investigation of particles' transport, deposition and resuspension under unsteady conditions in constructed stormwater ponds, Environ. Sci. Eur. 32 (2020) 1–17.
[44] F.R. Menter, Two-equation eddy-viscosity turbulence models for engineering applications, AIAA J. 32 (8) (1994) 1598–1605.
[45] ANSYS Inc., ANSYS fluent theory guide, 2022, Release 2022 R1, Canonsburg, PA, USA.
[46] A. Aboelezz, M. Beltran, M.J. Hargather, M. Hassanalian, P. Roghanchi, Comprehensive design and performance validation of a wind tunnel for advanced respirable dust deposition investigations, J. Hazard. Mater. 478 (2024) 135516, http://dx.doi.org/10.1016/j.jhazmat.2024.135516.